The effect of secondary crystallization on crystallization kinetics – Polyethylene terephthalate revisited

Chen, Ziyu; Hay, James N.; Jenkins, Michael J.

DOI:
10.1016/j.eurpolymj.2016.05.028

Document Version
Peer reviewed version

Citation for published version (Harvard):
Chen, Z, Hay, JN & Jenkins, MJ 2016, 'The effect of secondary crystallization on crystallization kinetics – Polyethylene terephthalate revisited', *European Polymer Journal*, vol. 81, pp. 216-223. https://doi.org/10.1016/j.eurpolymj.2016.05.028

The Effect of Secondary Crystallization on Crystallization Kinetics – Polyethylene Terephthalate Revisited

by

Ziyu Chen, James N. Hay* and Michael J. Jenkins,

The School of Metallurgy and Materials,

College of Physical Science and Engineering

The University of Birmingham,

Edgbaston,

Birmingham B15 2TT, UK

Figures: - 9

Tables: - 4

*Corresponding Author

Tel: +44 121 414 4544 Fax: +44 121 414 5232

E-mail address: j.n.hay@bham.ac.uk. [J. N. Hay]

The Effect of Secondary Crystallization on Crystallization Kinetics – Polyethylene Terephthalate Revisited

by

Ziyu Chen, James N. Hay* and Michael J. Jenkins,

The School of Metallurgy and Materials, College of Physical Science and Engineering ,The University of Birmingham, Edgbaston, Birmingham B15 2TT, UK

Abstract.

The possibility that two concurrent crystallization processes occurring during the crystallization of polymers may account for anomalous fractional values of the Avrami exponent, of no theoretical significance, is reconsidered using data from the recent evaluation of the kinetics of crystallization of poly (ethylene terephthalate) which placed emphasis on evaluating the secondary crystallization stage . In general constant n values in excess of that expected for the crystallization mechanisms could readily be interpreted in terms of the additional crystallinity developed by the secondary process and these values increased commensurate with the rate constant of secondary crystallization.

The difference in mechanisms of primary and secondary arises from differences in the mechanism of chain segment diffusion by reptation and the free energies of nucleation of the two growth steps.

Keywords:

Crystallization kinetics

Secondary crystallization

Reptation

Nucleation

1. Introduction

In a previous publication [1] the kinetics were analyzed as two consecutive processes, attributed to primary and secondary crystallization, obeying Avrami equations with n values of 2 and 1 respectively , i.e.

$$X_t = X_{p,\infty}\{1- \exp-(Z_p(t-t_i)^2\} + X_{s,\infty}\{1 -\exp-Z_{s,\infty}(t - t_i)\} \qquad [1]$$

where $X_{t.}$, $X_{p,\infty}$ and $X_{s,\infty}$ are the fractional crystallinities at time t, at the end of the primary and secondary processes. Z_p and Z_s are composite rate constants involving nucleation and crystal growth for each process, t_i the induction time and integer constants reflecting the dimensions in which crystal growth occurred and the nucleation characteristic, i.e. sporadic or pre-determined. This was consistent with the growth and impingement of disc spherulites confined by the thickness of the film samples and one dimensional thickening of the lamellar structural units of the spherulites.

It has become increasingly apparent from studies on the effect of ageing on the melting point, m.pt., of poly(ethylene terephthalate), PET, [1-3] and poly(ϵ-caprolactone), PCL, [4,5] that a different mechanism is required to explain secondary crystallization, in particular the dependence of the fractional crystallinity and the increase in lamellae thickness with the square root of time, the increase in the rate constant and extent of secondary crystallization with temperature. This results in secondary crystallization and also ageing becoming more important at higher temperatures and argues against it being a nucleation controlled process for which the rate constant should decrease with increasing temperature, in line with its dependence on the degree of supercooling..

It was concluded that secondary crystallization was due to small segments of the chain being incorporated as out growths on the “fold surface” of the lamellae on the time scale of local segmental mobility and so independent of chain entanglements. Since it has been observed that the thickness of the lamellae is thicker towards the centre of the spherulite than at the outer boundary, secondary crystallization must develop as soon as the lamellae has formed and proceed along with and beyond the primary process [6].

In this paper the kinetics of secondary crystallization have been incorporated into the Avrami equation and used to re-interpret the kinetics of isothermal crystallization of PET as previously measured [1] and to interpret the constant non-integer values of n observed.

2. Experimental

Polymer characteristics and experimental procedures are as outlined in detail elsewhere [1].

3. Results and Discussion

3.1. Derivation of Kinetic Equation.

Several kinetic equations have been derived to follow the development of secondary crystallization with time. Most authors consider that it obeys an Avrami equation with n=1.0 due to a 1-dimension increase in thickness of the lamellae with impingement on adjacent lamellae [7, 8]; this leads to a dependence of the logarithm of the fractional crystallinity on time and cannot account for the observed dependence on the logarithm of time. It also gives a poor fit to the overall dependence of crystallinity with time.

Recently we have observed that during the secondary crystallization of PET and PCL [1-5] there is an increase in lamellae thickness by local diffusion of the chain segments on to the growth face and that the fractional crystallinity, $X_{s,t}$, increases with the square root of the crystallization time. If it is assumed that secondary crystallization occurs within the boundaries of the spherulites, and develops proportional to the extent of primary crystallization, $X_{p,t}$, then the total fractional crystallinity is

$$X_t = X_{p,t} + X_{s,t} \qquad (2).$$

Since from the Avrami equation

$$X_{p,t} = X_{p,inf}(1 - \exp\text{-}Z_p t^n) \quad (3)$$

And in line with experimental observation,

$$X_{s,t} = X_{p,t}\, k_s\, t^{½} \quad (4)$$

and $$X_t = X_{p,inf}\,(1\text{-}\exp\text{-}Z_p t^n)\,(1+ k_s\, t^{1/2}) \quad (5)$$

where Z_p is a composite rate constant incorporating nucleation and growth, n the Avrami exponent for primary crystallization and k_s the rate constant for diffusion controlled growth of the secondary process. The extent of secondary crystallization is further limited by the value of $X_{p,t,}$ to regions of the sample already confined within the boundaries of the spherulite.

At values of $X_t > X_{p,\infty}$ the primary process has ceased and the exponential function in eq.3 is equal to zero. The increase in fractional crystallinity with time is then,

$$X_{s,t} / X_{p,inf} = (1+ k_s\, t^{1/2}) \quad (6)$$

In order to confirm the dependence of $X_{s,t}$ on $t^{/1/2}$ the data determined previously [1] was analyzed after the primary process had ended and plots of $X_{s,t}/X_{p,inf}$ against $t^{1/2}$ were linear with intercepts of 1.00 and slope of k_s see Figure 1. These parameters for the secondary crystallization are listed in Table 1 as a function of crystallization temperature. The degree of fit of the data was gauged from the sums of the squares of the residuals, R^2, which were close to 1.00. There was a general trend for k_s to increase with temperature consistent with diffusion control of secondary

crystallization and the thermal activated process obeying an Arrhenius dependence on temperature, i.e.

$$k_s = A. \exp (-\Delta E/RT_c) \quad (7)$$

where A is a pre-exponential factor, ΔE the activation energy for viscous flow, R the gas constant and T_c the crystallization temperature.

The activation energy was determined to be 108±40 kJ mol $^{-1}$, see Figure 2. This compares with 95±10 kJ mol^{-1} determined previously for the activation energy of diffusion for PET [3]. The large uncertainty in the activation energy reflects the small temperature range studied and the small change in $X_{s,t}$ associated with secondary crystallization.

Table 1. Secondary Crystallization Rate Parameters

Crystallization Temperature / ^{o}C	Fractional Crystallinity $X_{p,\infty}$	Rate Constant k_s /min$^{-1/2}$ x 10 ^{3}	Degree of Fit R^2
240.0	0.26	21.8 ± 2.0	0.989
238.0	0.20	18.4 ± 1.5	0.993
236.0	0.29	11.7 ± 1.0	0.993
234.0	0.29	13.0 ± 1.0	0.986
232.0	0.30	12.1 ± 1.0	0.988
230	0.35	11.2 ± 1.0	0.994

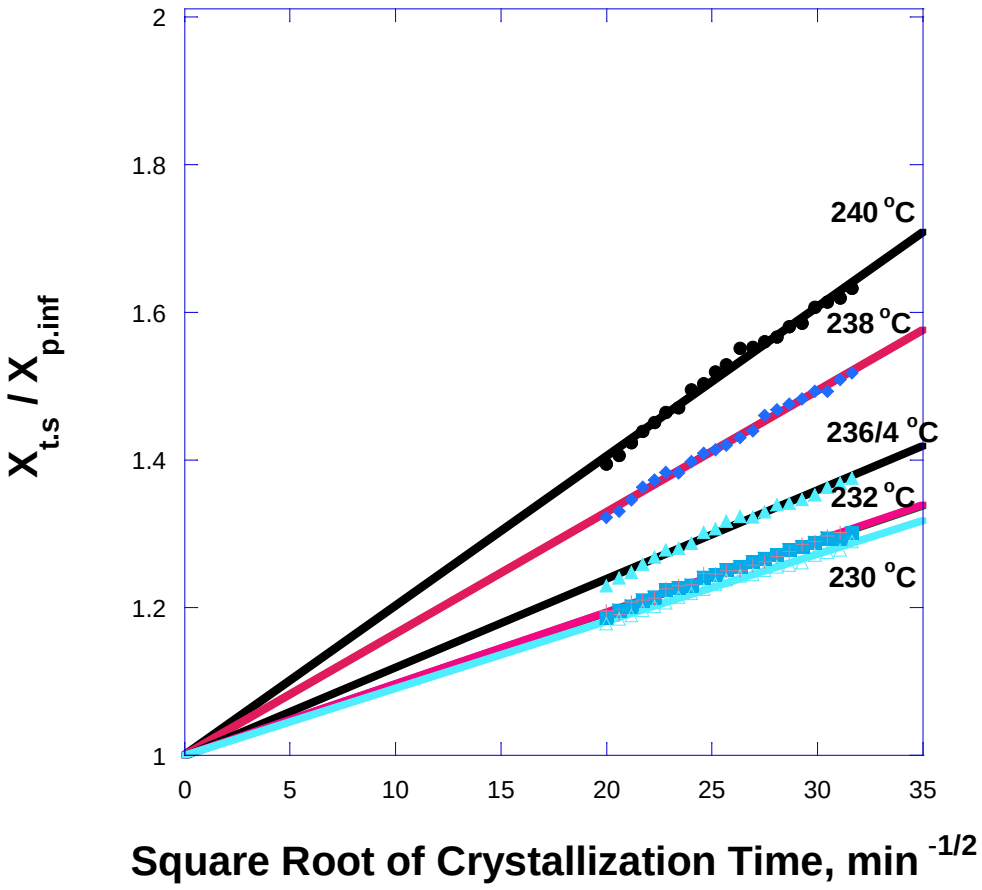

Figure 1. Dependence of the secondary fractional crystallinity on the square root of time.

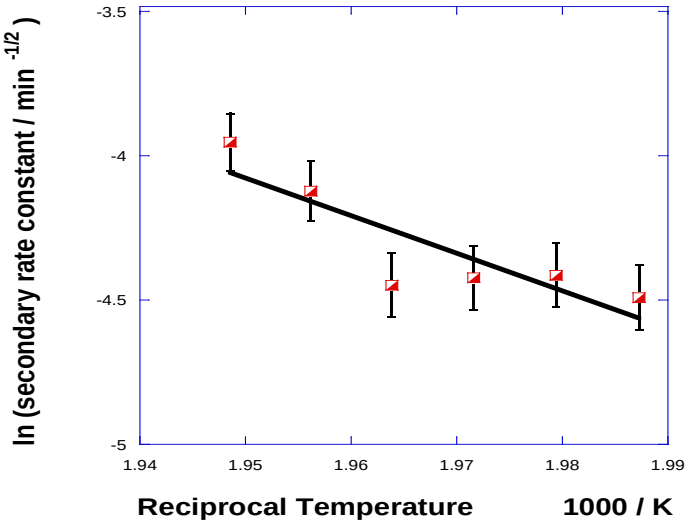

Figure 2. Arrhenius plot of secondary rate constants.

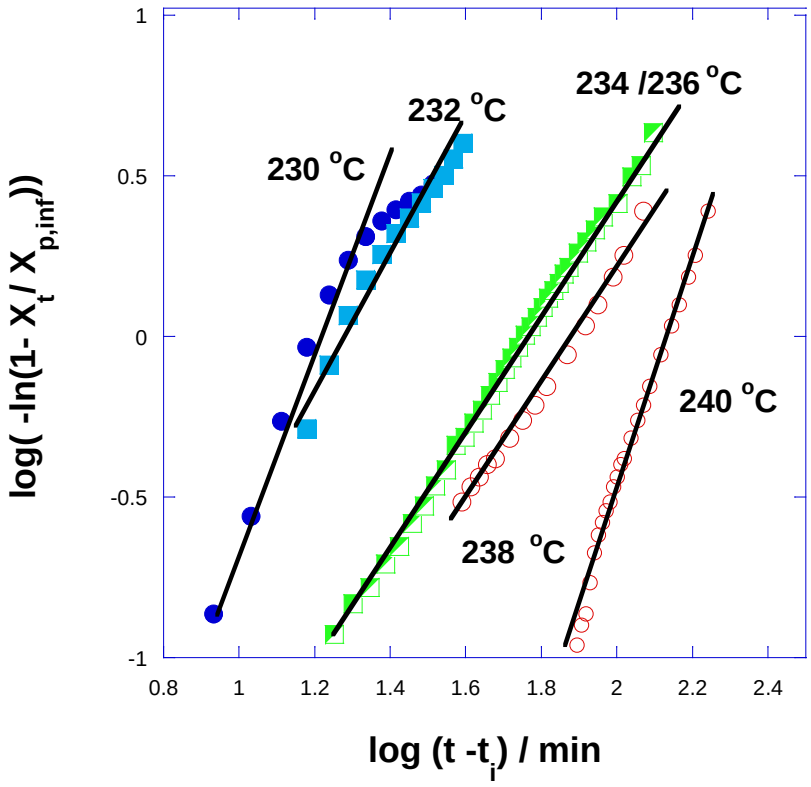

Figure 3. The determination of n values.

Table 2. Crystallization Rate Parameters.

Crystallization Temperature / ^{o}C	**Exponent n ± 0.1**	**Half Life ($t_{1/2} - t_i$)/ min**	**Induction Time / min**	**R^2**
240	**2.22**	**95**	**55**	**0.993**
238	**2.14**	**55**	**24**	**0.998**
236	**2. 12**	**38**	**20**	**0.990**
234	**2.13**	**20**	**9**	**0.993**
232	**2.16**	**18**	**2**	**0.973**
230	**2.20**	**12**	**-2**	**0.969**

The crystallization rate parameters, as listed in Table 2, were determined by means of equation 3 using the value of $X_{p,\infty}$ determined above and t_i the time to the first detectable onset of crystallization. The half-lives were taken to be the time at which $X_t = X_{p,inf}/ 2$ and Z_p calculated from

$$Z_p = 0.693 / (t_{1/2})^2 \qquad (8)$$

The value of n was determined from the slope of the linear plots of log $(-\ln (1-X_t/X_{p,\infty})$ against log $(t-t_i)$, see Figure 3, since,

$$\log (-\ln (1- X_t/ X_{p,\infty}) = n \log (t- t_i) + \log (Z_p) \qquad (9)$$

. The relative goodness of fit gauged from the R^2 value, as 0.97-0.99. The n values were in the range 2.2 ±0.1 consistent with the heterogeneous nucleation of discs of

constant thickness [9]. Although n values were all fractional they were close to but above the expected integral value of 2.0.

3.2 Application to crystallization rate data.

The variations in the fractional crystallinity with time, defined by equation 4 and using the listed parameters, $X_{p,\infty}$, t_i and k_s, were calculated and compared directly with the experimentally determined values, see Figure 4. The Avrami exponent, n, was selected to be 2.0 as required by the model of heterogeneously nucleated discs and Z_p calculated from the half-life; there were thus no adjustable parameters. The calculated fractional crystallinities are compared with the experimentally determined values in Figure 4 but the accuracy of the fit to the data was more clearly seen from their differences (between experimental and calculated fractional crystallinities) measured over the entire temperature range, see Figure 5. The fit of the data was better than ±0.02 initially and ±0.005 finally and compares well with the error in measuring X_t experimentally of ±0.005 [1].

The calculated X_t v, t data is separated into the component parts due to primary and secondary crystallization in Figure 6 from which it can be seen that the secondary crystallization contributed substantially to the overall crystallinity, as much as 20% at the end of the primary process and about 30% finally. In order to determine the effect of this overlap on the measured value of the Avrami exponent the calculated data was

analyzed by the same procedure adopted above and the n values determined from the slope of the plot of $\log(-\ln(1-X_t/X_{p,inf})$ against log(t), see Table 3. In every case the n

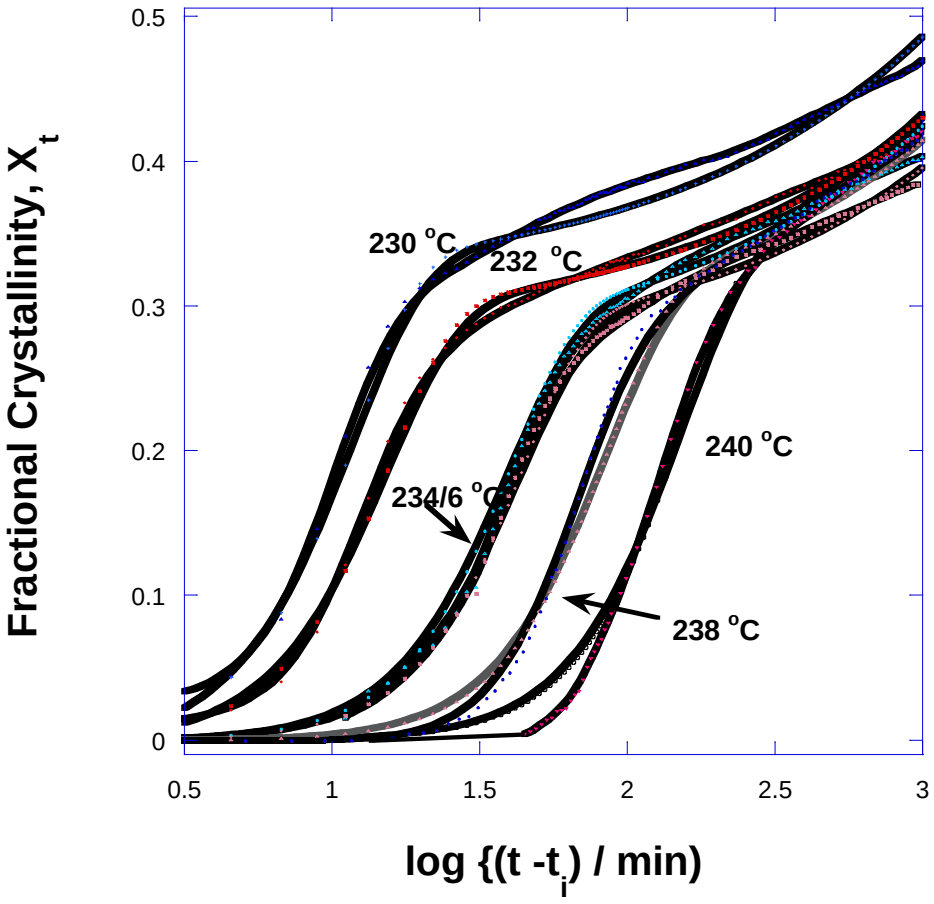

Figure 4. Comparison of the experimental and calculated fractional crystallinities with log crystallization time.

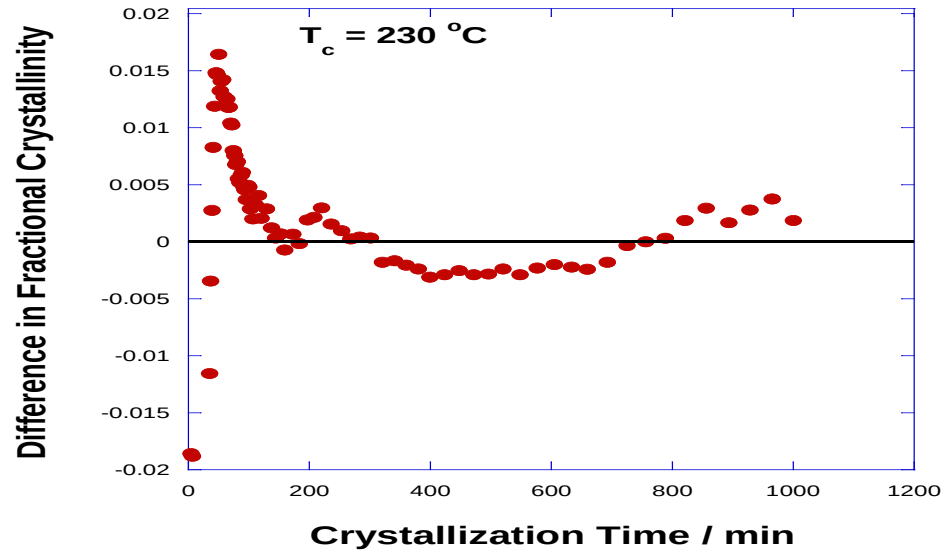

A.

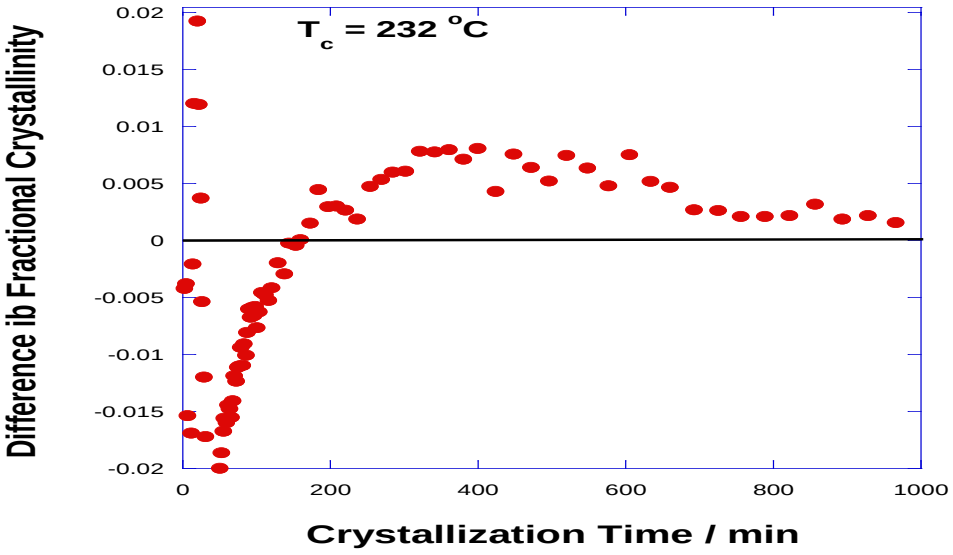

B.

Figure 5. The difference between observed and calculated fractional crystallinities.

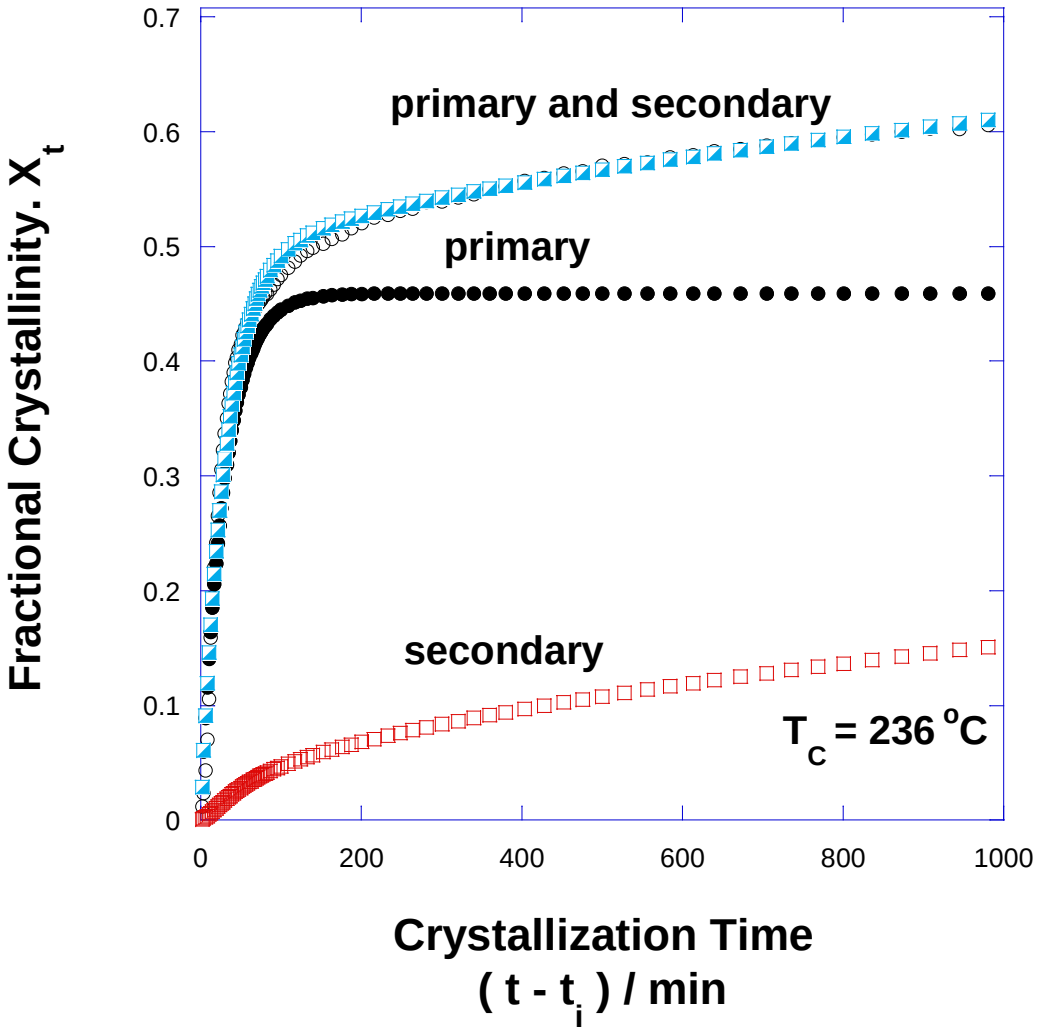

Figure 6. The separation of the calculated fractional crystallinity into primary and secondary components.

Table 3. The Effect of Secondary Crystallization on the n Value.

Crystallization Temperature / ^{o}C	230	232	234	236	238	240
n Value expt.± 0.10	2.27	2.16	2.13	2.20	2.14	2.12
n Value Calc.± 0.10	2.16	2.14	2.10	2.05	2.16	2.20

values were greater than the value adopted. This increase was attributed to the contribution the secondary process made to the development of crystallinity during the primary stage.

Clearly the time-dependence of $X_{p,t}$ and not X_t should be analyzed since it alone follows an Avrami dependence. From equations 3 to 5, it can be shown that

$$X_{p,t} = X_t/(1+ k_s t^{1/2})$$

And also $$X_{p,t} = X_{p,inf}(1 – \exp\text{-}Z_p t^n)$$

Plots of $\log(-\ln(1- X_t/ \{X_{p,inf} (1+ k_s t^{1/2}) \}))$ against log (t) for the original experimental data were linear with slopes corresponding to an n value of 2.00±0.05, see Figure 7 and Table 4. Measure of the goodness of fit of the least square analysis, R^2, were all better than 0.99. The rate parameters for the primary crystallization are listed in Table 4. They are consistent with the growth of disc-like spherulites confined

to the thickness of the film and nucleated with heterogeneous nuclei as the mechanism for primary crystallization.

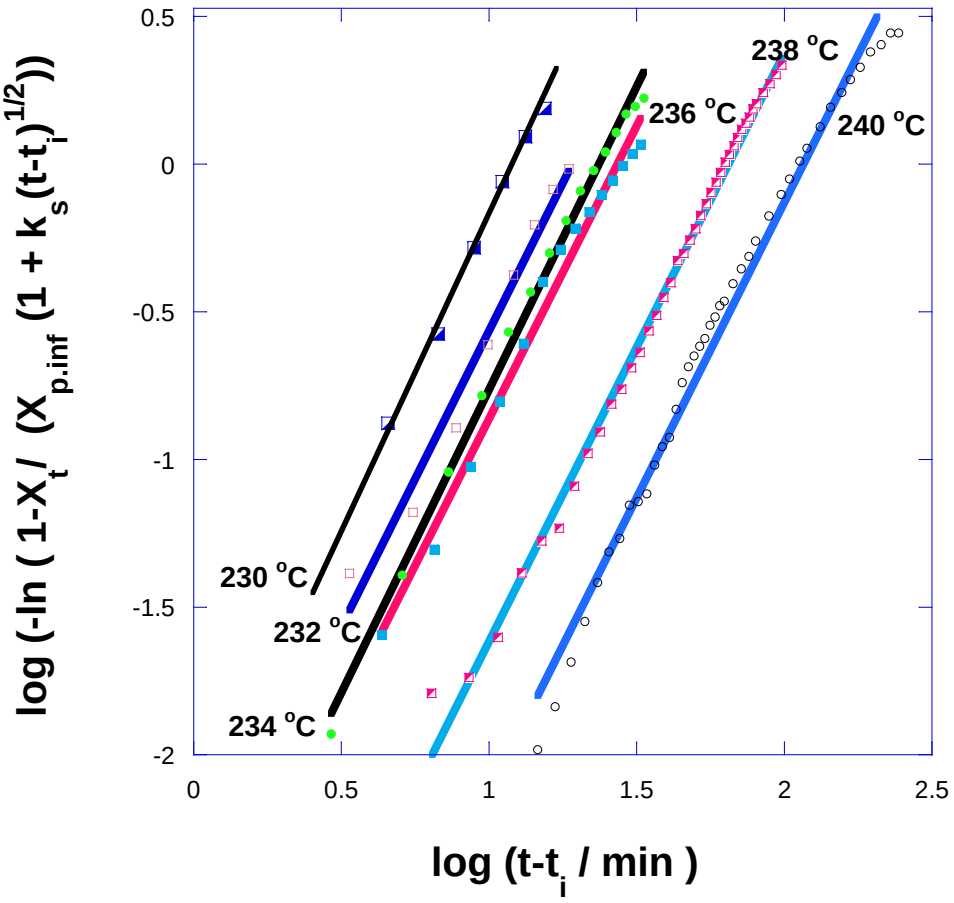

Figure 7. Analysis of the primary fractional crystallinity.

Table 4. Primary Crystallization Rate Parameters

Crystallization Temperature / ^{o}C	Fractional Crystallinity $X_{p,inf}$	n Value ± 0.03	-log(Z_p)	Degree of Fit R^2
240.0	0.26	2.00	4.13	0.99
238.0	0.20	1.99	3.61	0.99
236.0	0.29	1.98	3.31	0.99
234.0	0.29	2.05	2.82	1.00
232.0	0.30	2.00	2.57	0.98
230.0	0.35	2.04	2.26	1.00

3.3 The effect of secondary crystallization on n value.

In order to determine the effect of secondary crystallization on the observed value of n, the secondary rate constant, k_s, was systematically altered while the rate parameters of the primary process were kept constant. The fractional crystallinity was calculated using equation 4 with $X_{p,inf}$ = 0.50 and a half-life of 200 min. Integer values, 2, 3, and 4, of n were chosen to conform to the crystallization model of expanding spheres and discs homogeneously and heterogeneously nucleated as adopted by Avrami [9]. The rate constant for secondary crystallization was changed systematically from 0.0 to 3.0 x 10^{-2} $min^{-1/2}$ to limit the extent of secondary crystallization to less than half the total crystallinity. The resulting development of secondary crystallinity, X_{st}, with time can be seen in Figure 7 for n=3.0. The effect

of increasing the rate constant increases the contribution of secondary crystallization to the initial development of crystallinity previously assigned to the primary process; it is clear that as the rate constant increases secondary crystallization makes a larger contribution to the overall crystallinity during the initial stages and dominates after the end of the primary process. Similar conclusions were reached using n=2.0 and n=4.0.

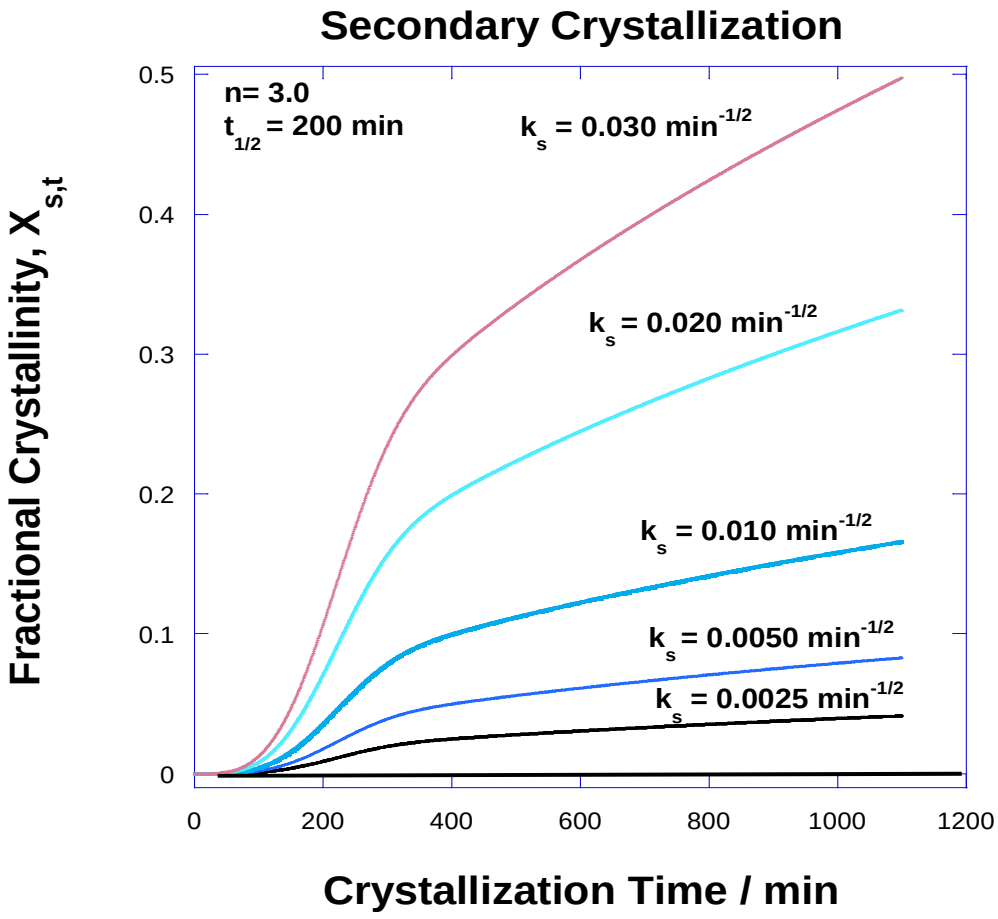

Figure 8. The development of secondary crystallization with time.

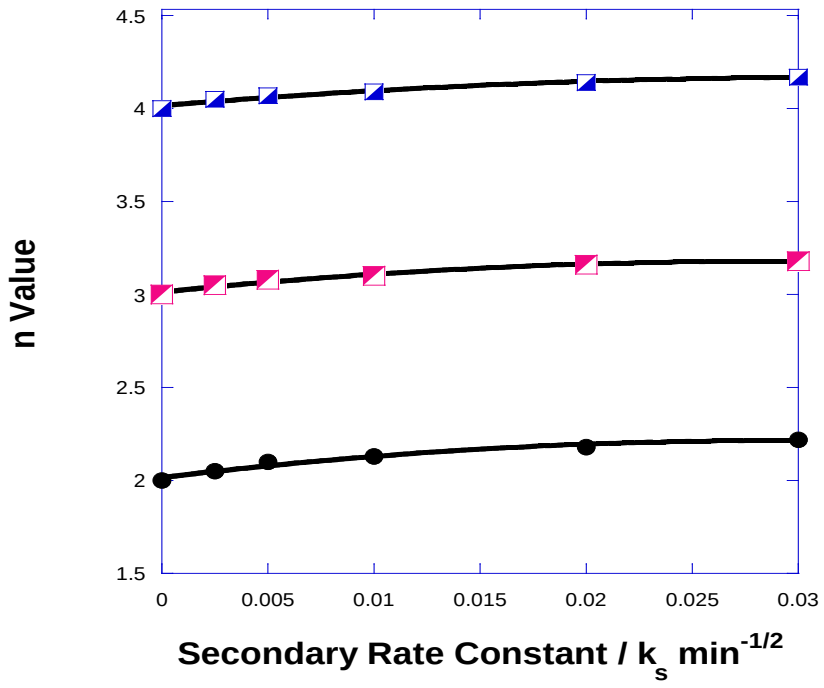

Figure 9. Effect of the secondary rate constant on the n value of the primary crystallization.

The values of the exponents, n, were calculated from the crystallization-time data up to $X_{p,inf}$ in order to determine the effect of the increasing amounts of secondary crystallization on the fit of the Avrami equation to the primary process. The values of n were again determined from the slopes of plots of log (-ln ($1-X_t/X_{inf}$)) against log t over the range of rate constants, k_s and in every case n was constant and the degree of fit as determined by R^2 was above 0.99 but fractional with values which increased from n to n+0.3 with k_s, see Figure 8. These values of n are in keeping with those determined previously and listed in table 3. The contribution to the fractional crystallinity during the primary stage of development due to secondary

crystallization is sufficient to account for the increase in n value above that predicted by Avrami [9}.

4.0 Conclusions.

Two different crystallization mechanisms are observed in the crystallization of polymers which are associated with primary and secondary crystallization and are readily distinguished by their very different time dependence; the first increases with an exponential dependence on time and the second with the square root of time. This implies that different crystallization mechanisms are involved. There is further evidence from electron microscopy [6] and melting studies [2,5] that the lamellae thicken progressively from when they first develop. Secondary crystallization develops from the onset of crystallization, increases as the primary crystallinity increases and eventually dominates after the end of the primary stage. Incorporating a rate expression into the Avrami equation to account for the additional crystallinity produces constant fractional values for the exponent n. The exponent increases from the expected integer value in proportion to the increase in secondary crystallization and can account for some of the fractional values observed in the crystallization of most polymers.

The primary process is considered to be due to the growth of spherulites whose radial growth is linear with time up to impingement with adjacent spherulites. The

growth rates exhibit a bell-shaped dependence with temperature as explained by Hoffman et al [10] in terms of diffusion and nucleation

This is not the case with secondary crystallization since the rate increases with the square root of time and the rate constant increases with temperature as diffusion rather than nucleation controlled phase separation. The difference between the two mechanisms lies in the thermodynamics of the critical size nucleus and in particular the size of the growth nucleus as outlined previously [1.2]. Secondary crystallization occurs by the extension of the "fold surface" into the melt and there is no additional fold surface created in extending the lamellae. Accordingly the fold surface free energy term is not involved in determining the free energy of the critical size nucleus, ΔG_f. Accordingly, the nucleus is greatly reduced in size and the dimensions of the growth surface become less than the distance between adjacent entanglements of the chain in the melt. The incorporation of the chain segments on to the crystal growth face is that of reptation within the virtual tube between entanglements and is dependent on the square root of time. The substantial reduction in ΔG_f results in secondary crystallization being diffusion rather nucleation controlled.

Acknowledgements

We are indebted To Mr. Frank Biddlestone for technical support**.**

References.

[1] Chen Z, Hay JN, Jenkins MJ, Europ. Polym. J 2013: 49, 1722.

[2]. Chen Z, Hay JN, Jenkins MJ, Europ. Polym. J 2013:49, 2697.

[3]. Chen Z, Jenkins MJ, Hay JN, Europ. Polym. J 2014: 50, 235.

[4]. Phillipson K, Jenkins MJ, Hay JN, Polym. Inter 2015: 64, 1695.

[5]. Phillipson K, Jenkins MJ, Hay JN, J Therm Anal Calorim 2016: 123, 149. [6].El Maaty MIA, Bassett DC, Polymer. 2005:46;8682.

[7]. Hillier IH J Polym Sci A 1965;3:3067.

[8]. Hay JN, Booth A, Brit. Polym. J 1972:4; 19

[9]. Avrami MJ, J Chem Phys 1939;7:1103.

[10].Hoffman, JD Frolen IJ, Ross GS, Lauritzen JL,jr., J Res Nat Bur Standards, 79A: 671.